Supplementary Information (SI) for Journal of Materials Chemistry B.

Electronic Supplementary Information (ESI)

Phase-separated structures of tunable thermoresponsive and matrix polymers for large-scale temperature monitoring coatings

Risako Shibata,[a] Satoru Matsuda,[b] Hirofumi Kawakubo,[b] Hiroaki Imai,[a] Yuya Oaki*,[a]

[a] Department of Applied Chemistry, Faculty of Science and Technology, Keio University, 3-14-1 Hiyoshi, Kohoku-ku, Yokohama 223-8522, Japan.

[b] Department of Surgery, School of Medicine, Keio University, 35 Shinanomachi, Shinjuku-ku, Tokyo 160-8582

E-mail: oakiyuya@applc.keio.ac.jp

Contents

Experimental methods

Preparation of the phase-separated structures. The following regents were used as purchased without purification: 10,12-pentacosadiynoic acid (PCDA, TCI, 97.0 %) as a DA monomer, *p*-xylylenediamine (*p*-Xy, 99 %) and L-lysine (L-Lys, 97 %) as guests, poly(allylamine) (PAlyAm, Aldrich M_W 65,000, 10 wt% aqueous solution or 17,000, 20 wt% aqueous solution) as a matrix polymer. The precursor solution containing 120 mg PCDA was prepared with ethanol (36.0 cm^3). After a trace amount of the polymerized precipitate was removed with filtration, the guests, such as 22.3 mg *p*-Xy for or 48.3 mg for L-Lys, were added to the solution. Then, PAlyAm aqueous solution (180 mm^3 for 20 wt-% PAlyAm aqueous solution and 360 mm^3 for 10 wt-% PAlyAm aqueous solution) was added to the precursor ethanol solution. The precursor solution containing the host, guest, and matrix polymer was set in a sonic bath for 60 min.

The bulk sample was prepared by the evaporation of the solvent from the precursor solution. The spray coating was carried out throughout substrates, 3 cm-square except a paper-based sticker, vertically set on the table with a distance ca. 20 cm from the bottle containing the precursor solution. The coating solution (5 cm^3) was sprayed and then the substrate was dried at room temperature for 10 min. This spraying and drying processes were repeated totally three times using total 15 cm^3 of the precursor solution. The resultant coatings of the PCDA monomer were polymerized with the irradiation of UV light (6 W, As-one handy UV lamp, 254 nm) for 10 s. The same coating and polymerization methods were applied to substrates, such as polyurethane (PU), polyethylene (PE), polypropylene (PP), silk cloth, PE cloth, polystyrene (PS), copper foil, stainless steel, and tubular silicone. The coating on a paper-based sticker (5 × 6 cm) was carried out using 25 cm^3 of the precursor solution. The sticker was cut after the polymerization and then attached on the shaft of an energy device.

The reference samples of the phase-separated structures were prepared by changes of the guest molecules and matrix polymers. The layered PDA was prepared using the different guests instead of *p*-Xy, such as 4-methoxybenzylamine (OMeBA, TCI 97.0 %), 4-fluorobenzylamine (FBA, TCI 98.0 %), 4-methylbenzylamine (MeBA, TCI 98.0 %), and benzylamine (BA, TCI 99.0 %), with PAlyAm matrix polymer. The molar ratio of these guests and PAlyAm to PCDA were adjusted to both 1.00. The experimental procedure was the same as that of *p*-Xy. In addition, the layered PDA was prepared using the different matrix polymers, such as polymethyl methacrylate (PMMA, Aldrich, M_W = 120,000), poly(4-viynlpyridine) (4PVP, Aldrich, M_W = 60,000), and poly(acrylic acid) (PAcA, Aldrich M_W = 250,000) instead of PAlyAm (Fig. S5).

The concentration and methods were the same as those of PAlyAm. These samples were spray-coated on a cleaned glass slide.

Structure characterization. The interlayer distance (d_0) was measured by X-ray diffraction (XRD, Bruker D8-Advance). The changes in the states of functional groups in the interlayer space were analyzed by Fourier-transform infrared (FT-IR, JASCO FT/IR-4200) spectroscopy. The polymerization behavior was analyzed using Raman spectroscopy (Renishaw, InVia Raman) with irradiation of excitation light (785 nm) for the measurement and UV light (254 nm) for the polymerization. The thermoresponsive structure changes were studied by differential scanning calorimetry (DSC, Shimadzu DSC-60 plus) under nitrogen atmosphere. UV-Vis spectra was measured using a spectrophotometer (Shimadzu, UV-2600i) equipped with a temperature controlling unit (S.T. Japan). These XRD, FT-IR, Raman, DSC, and UV-Vis analyses were carried out using the bulk samples. The morphologies were observed by scanning electron microscopy (SEM, Hitachi S-4700, JEOL JSM-7600F, Carl-Zeiss MERLIN VP compact) and optical microscopy (Olympus, BX51-FL). The samples were prepared by spray-coating on a cleaned silicon substrate and paper-based sticker.

Thermoresponsive color-changing properties. The spray-coated samples on the sticker were heated and cooled using temperature-controlled stages from 25 to 160 °C (Linkam, LNP94/2, 10002 with liquid nitrogen or As-One cool plate depending on the temperature range). The temperature was maintained for 30 s and then the photograph was taken using a smartphone (iPhone 12 Pro Max). R, G, and B values in the same area of the photographs were calculated using Image-J software. The red-color intensity (x) was calculated using (eq. S1), an international standard (ITU-R BT. 709), and (eq. S2). The relationship between temperature (T) and an increment of x (Δx) was summarized to study the color-changing properties.

$$\begin{bmatrix} X \\ Y \\ Z \end{bmatrix} = \begin{bmatrix} 0.4124 & 0.3576 & 0.1805 \\ 0.2126 & 0.7152 & 0.0722 \\ 0.0193 & 0.1192 & 0.9505 \end{bmatrix} \begin{bmatrix} R \\ G \\ B \end{bmatrix} \quad \ldots \text{(eq. S1)}$$

$$(x, y) = \left(\frac{X}{X+Y+Z}, \frac{Y}{X+Y+Z} \right) \quad \ldots \text{(eq. S2)}$$

The samples prepared using the other guest molecules and matrix polymers were characterized by the optical microscopy images. The samples coated on a glass slide were heated and cooled using a temperature-controlled unit (Linkam, LNP94/2, 10002) set on the stage of the microscope.

Temperature imaging using an energy device. The PAlyAm/PDA-L-Lys coated sticker was attached on the shaft of ultrasonic incision coagulation device. A sliced pork set on a temperature-controlled stage at 37 °C was cut using the device. The movie was taken during the simulated operation. The photographs were extracted from the movie to calculate the Δx value. The standard curve representing the relationship between T and Δx was prepared using the sticker device in the temperature range of 60–100 °C.

Structural analyses of PAlyAm/PDA-L-Lys and PDA-L-Lys

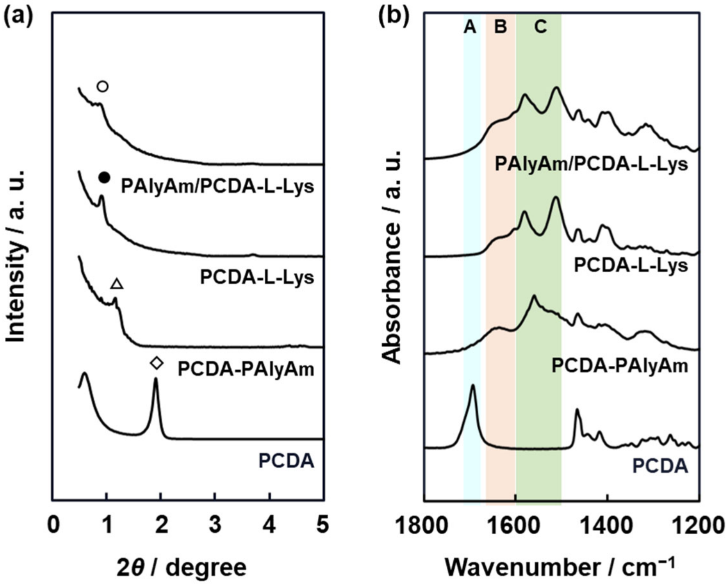

Fig. S1. XRD patterns (a) and FT-IR spectra (b) of PAlyAm/PCDA-L-Lys, PCDA-L-Lys, PCDA-PAlyAm, and PCDA.

Whereas the original PCDA had d_0 = 4.67 nm, the intercalated guests expanded d_0 to 6.24 nm for PCDA-L-Lys and 6.41 nm for PAlyAm/PCDA-L-Lys. The reference PCDA-PAlyAm showed d_0 = 5.57 nm. FT-IR spectra showed the same spectroscopic changes as observed for the intercalation of *p*-Xy, indicating the formation of PAlyAm/PCDA-L-Lys with the phase-separated structure.

Raman spectra

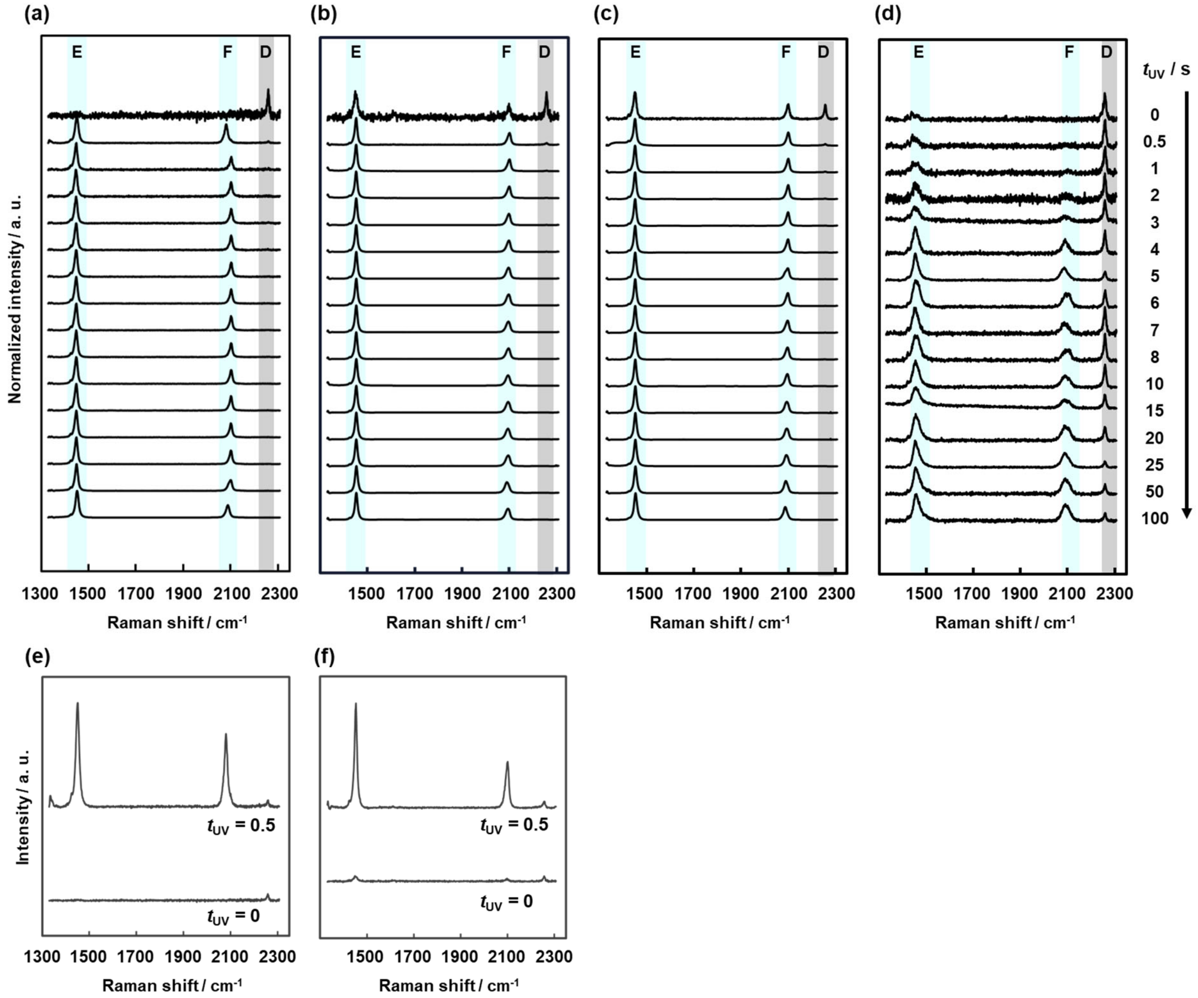

Fig. S2. Raman spectra of PCDA (a,f), PAlyAm/PCDA-*p*-Xy (b,e), PCDA-*p*-Xy (c), and PCDA-PAlyAm (d) with changes in t_{UV} within 0–100 s. (a–d) Normalized spectra. (e,f) Original data at t_{UV} = 0 and 0.5 s.

The intensity ratio of the peaks F (I_{poly}) to D (I_{mono}) ($R_I = I_{poly}/I_{mono}$) with increasing the UV-irradiation time (t_{UV} / s) was calculated using these spectroscopic data to study the polymerization behavior (Fig. 2d).

SEM images of PAlyAm/PDA-L-Lys

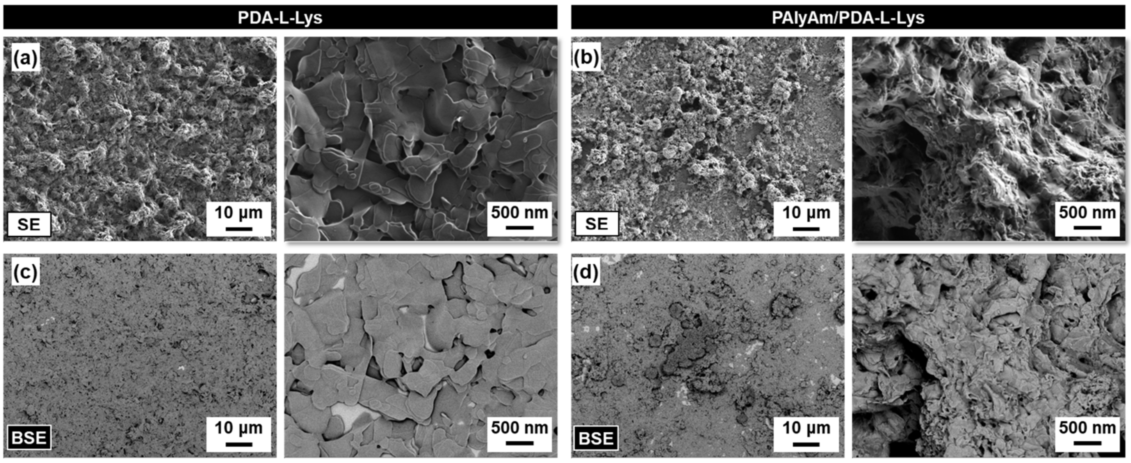

Fig. S3. Morphologies of the PDA-L-Lys (a,c) and PAlyAm/PDA-L-Lys (b,d) spray-coated on a silicon substrate. (a,b) SE images. (c,d) BSE images.

The plates of PDA-L-Lys around 500 nm in the lateral size were deposited on a silicon substrate (Fig. S3a). The size reduced for PAlyAm/PDA-L-Lys (Fig. S3b). The contrast differences were observed on the BSE image of PAlyAm/PDA-L-Lys (Fig. S3d), indicating the formation of the phase-separated structure. In contrast, no contrast difference was observed on the BSE image of PDA-L-Lys (Fig. S3c). The phase-separated structure containing the size-reduced PDA crystal was similar to that observed for PAlyAm/PDA-*p*-Xy (Fig. 3).

Phase-separated structures of the other combinations

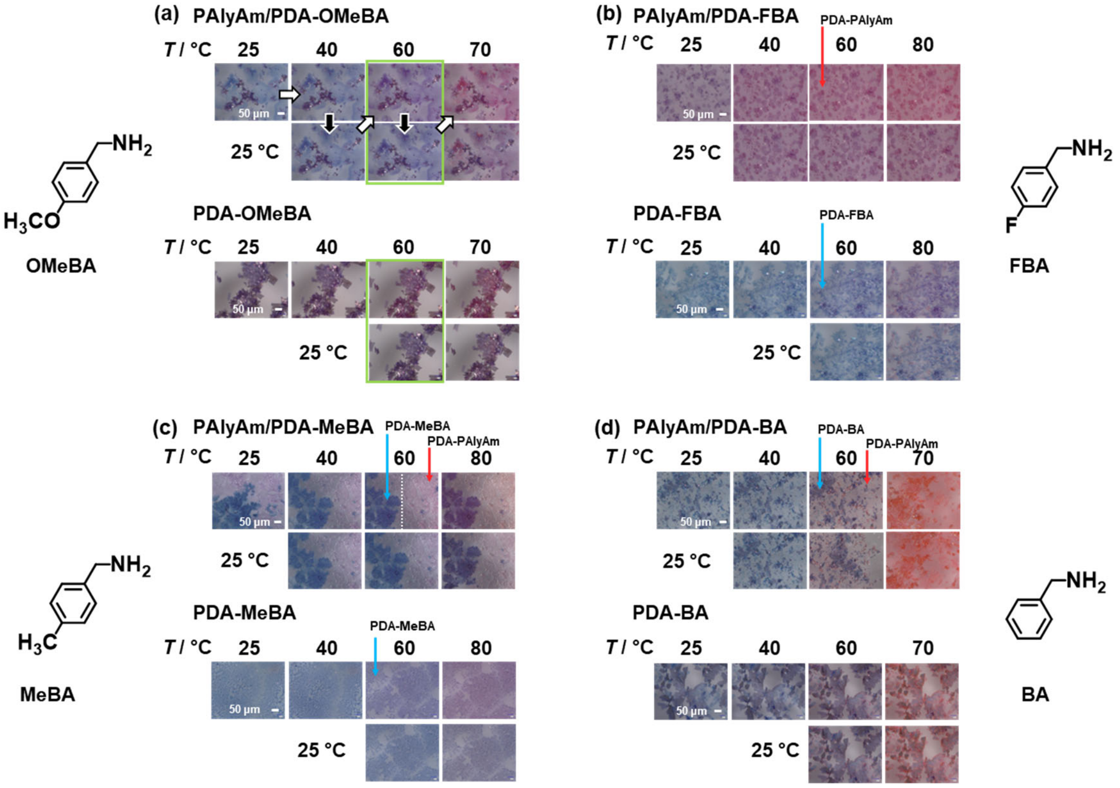

Figs. S4. Optical microscopy images of PAlyAm/PDA-OMeBA and PDA-OMeBA (a), PAlyAm/PDA-FBA and PDA-FBA (b), PAlyAm/PDA-MeBA and PDA-MeBA (c), and PAlyAm/PDA-BA and PDA-BA (d) with increasing temperature (upper) and subsequent cooling at 25 °C (lower).

The gust molecules and matrix polymers were changed to study formation of the phase-separated structures (Figs. S4 and S5). The layered PDA was prepared using the different guests instead of *p*-Xy, such as 4-methoxybenzylamine (OMeBA), 4-fluorobenzylamine (FBA), 4-methylbenzylamine (MeBA), and benzylamine (BA), with PAlyAm matrix polymer (Fig. S4). In these samples, the phase-separated structures were formed for PAlyAm/PDA-OMeBA (Fig. S4a). PAlyAm/PDA-OMeBA showed the thermoresponsive gradual color-change with the reversibility same as those of PDA-OMeBA. In contrast, PDA-PAlyAm was obtained from the precursor solution containing PCDA, PAlyAm, and FBA (Fig. S4b). The color-changing behavior of PAA/PDA-FBA was different from that of PDA-FBA. When MeBA and BA were used for the guests, PDA-PAlyAm and PDA-guest domains were separately observed (Fig. S4c,d). The phase-separated structures were not obtained for the FBA, MeBA, and BA guests. These guests are not preferentially intercalated in the interlayer space because of the weaker guest-guest interaction than that of *p*-Xy and OMeBA.

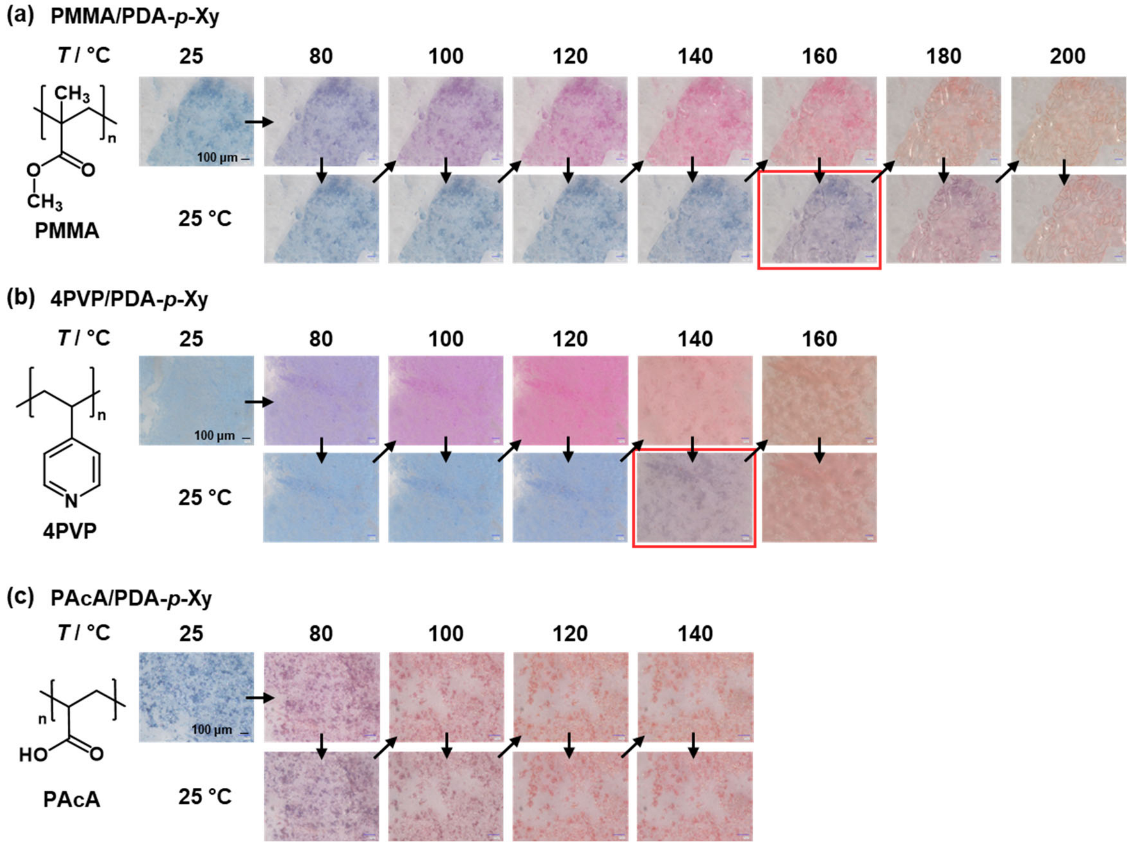

Fig. S5. Optical microscopy images of PMMA/PDA-*p*-Xy (a), 4PVP/PDA-*p*-Xy (b), and PAcA/PDA-MeBA (c) with increasing temperature (upper) and subsequent cooling at 25 °C (lower).

The layered PDA was prepared using the different matrix polymers, such as polymethyl methacrylate PMMA, 4PVP, and PAcA instead of PAlyAm (Fig. S5). The homogeneous coating with the thermoresponsive gradual color change with the reversibility similar to that of PDA-*p*-Xy was observed for PMMA/PDA-*p*-Xy and 4PVP/PDA-*p*-Xy (Fig. S5a,b). In contrast, such color changing behavior was not observed for PAcA/PDA-MeBA. The results imply that the formation of the phase-separated structures is achieved for PMMA/PDA-*p*-Xy and 4PVP/PDA-*p*-Xy. As PAcA has the interaction with *p*-Xy, the guest is not intercalated in the interlayer space.

Based on these results, the inert polymer is suitable as the matrix polymer. Moreover, the stronger interaction between the host and guest directs the preferential intercalation leading to formation of the phase-separated structures.

Large-scale coating on substrates

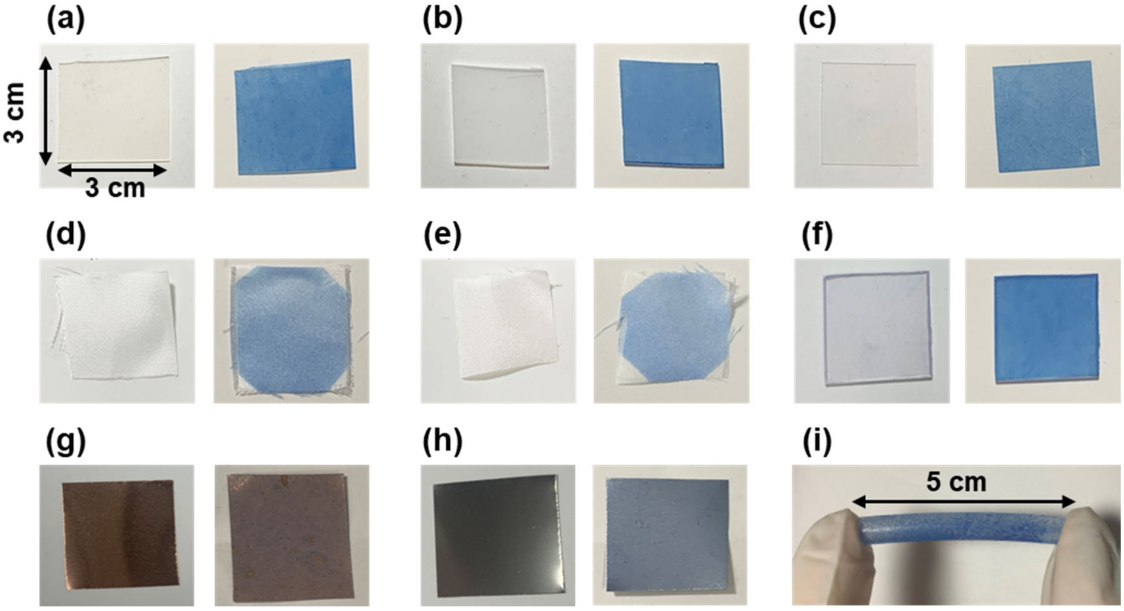

Fig. S6. Photographs of the bare substrates (left) and spray-coating of PAlyAm/PDA-*p*-Xy on the substrates (right). (a) Polyurethane (PU). (b) Polyethylene (PE). (c) Polypropylene (PP). (d) Silk cloth. (e) PE cloth. (f) Polystyrene (PS). (g) Copper. (h) Stainless steel. (i) Tubular silicone. The size was 3 × 3 cm for each substrate. The length of a silicone tube was ca. 5 cm.

PAlyAm/PDA-*p*-Xy was homogeneously coated by spraying the precursor solution on these substrates.

Coating of PAlyAm/PDA-L-Lys

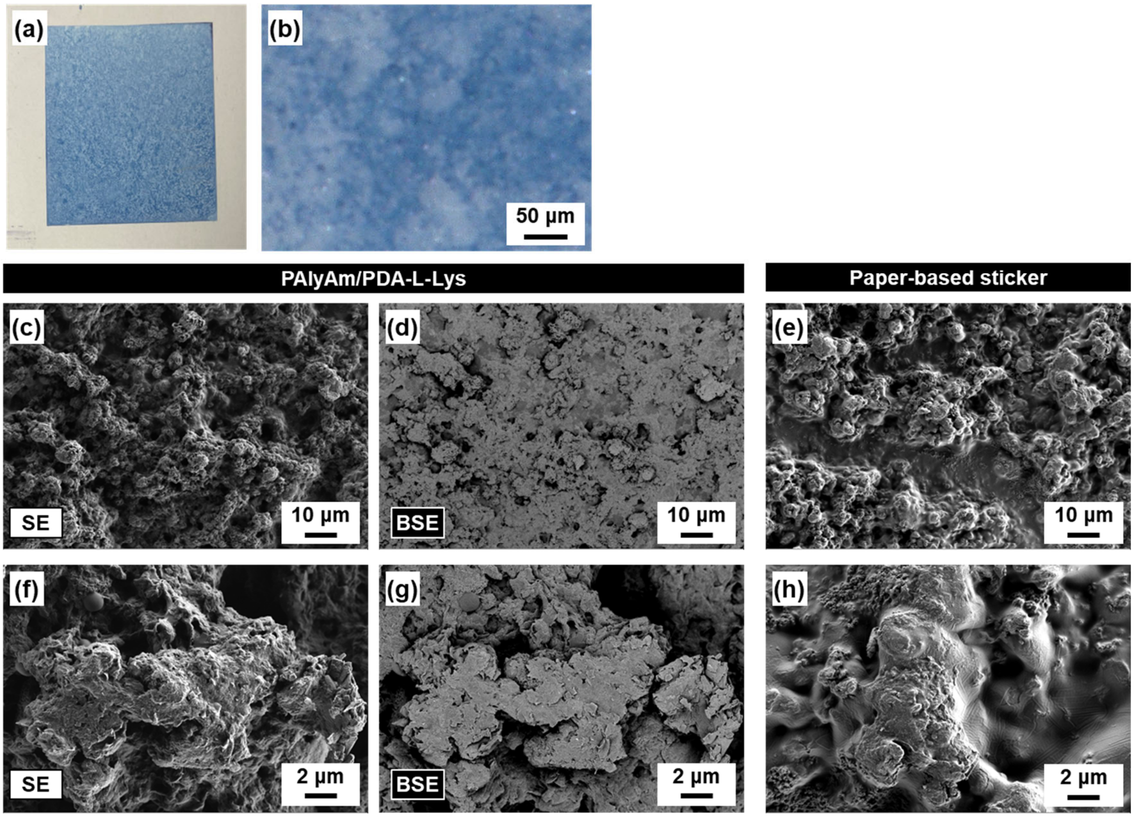

Fig. S7. Photograph (a), optical microscopy image (b), and SEM (SE and BSE) images (c–h) of PAlyAm/PDA-L-Lys coating on a paper-based sticker (a–d,f,g) and bare paper-based sticker (e,h).

The large-scale homogeneous coating was achieved on the paper-based sticker (Fig. S7).

Definition of Tstart, Tend, and Trev

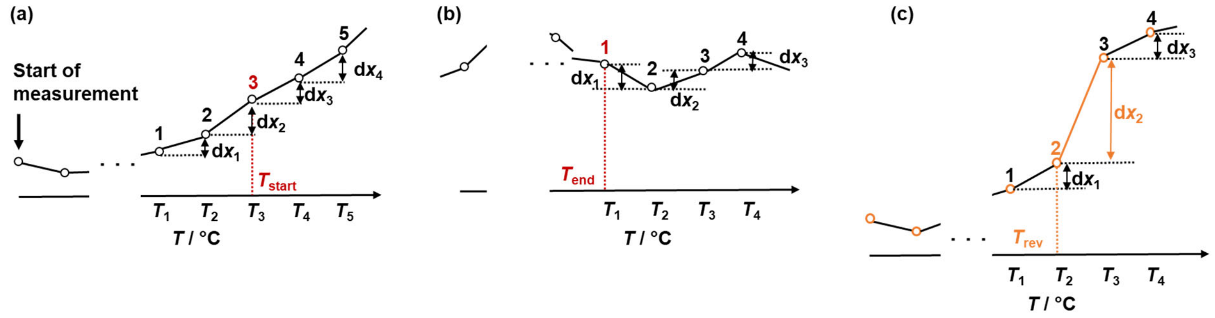

Fig. S8. Definition of T_{start} (a), T_{end} (b), and T_{rev} (c) in the relationship between T and Δx. The definition was same as that in our previous work.[36]

When the average increment of dx_1, dx_2 and dx_3 and the average increment of dx_2, dx_3 and dx_4 exceed 0.0005 and 0.001, respectively, T_3 is defined as T_{start} (Starting temperature of the color change) (Fig. S8a). When the differences in the average increment of dx_1 and dx_2 and the average increment of dx_2 and dx_3 are below 0.001, T_1 is defined as T_{end} (Ending temperature of the color change) (Fig. S8b). When the maximum of dx_n in the plots of the cooled state, such as dx_2 in Fig. S8c, is observed, T_2 is defined as T_{rev} (upper limit of the reversible color change) (Fig. S8c).

Cycle stability of the reversible color changes

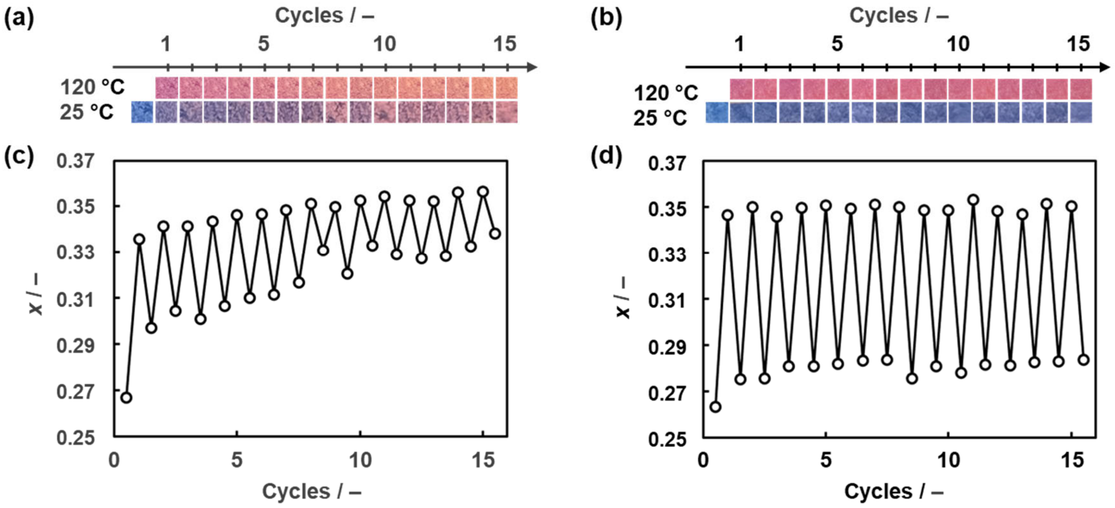

Fig. S9. Photographs (a,b) and relationship between the cycle and *x* (c,d) of PAlyAm/PDA-*p*-Xy (a,c) and PAlyAm/PDA-L-Lys (c,d).

Although PAlyAm/PDA-*p*-Xy showed the reversible color changes with heating and cooling (Fig. S9a,c), the red color was not completely recovered after the cycling. The deterioration is caused by evaporation of the intercalated *p*-Xy with heating. On the other hand, PAlyAm/PDA-L-Lys had the improved cycle stability for the reversibility (Fig. S9b,d).

UV-Vis spectra with changing temperature

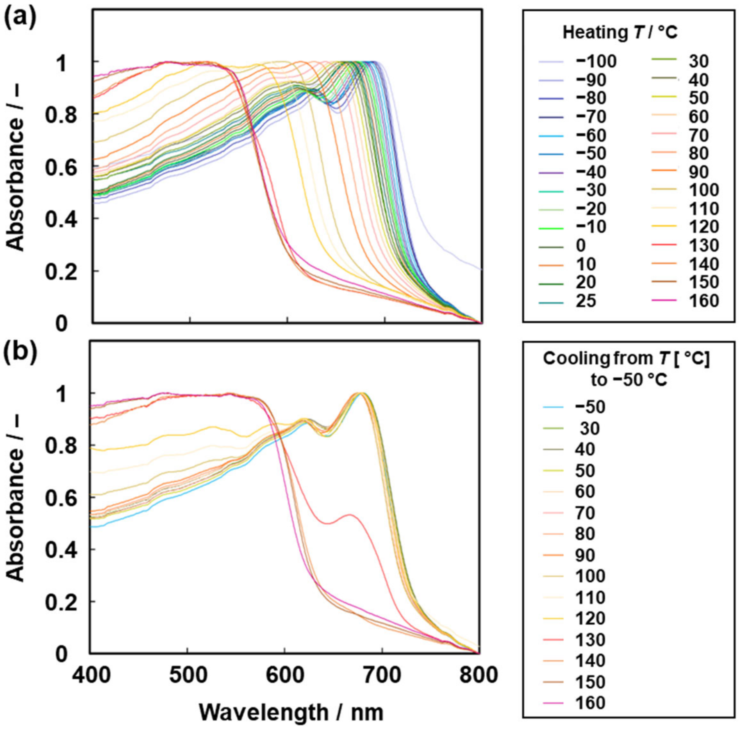

Fig. S10. Temperature-dependent UV-Vis spectroscopic changes of PAlyAm/PDA-*p*-Xy with heating at $T = -50$–160 °C (a) and subsequent cooling at −50 °C (b).

As temperature increased, the spectrum was gradually shifted to the shorter wavelength region (Fig. S9a). The peak position recovered to the original position after the subsequent cooling at $T < T_{\mathrm{rev}} = 140$ °C (Fig. S9b). The results indicate that PAlyAm/PDA-*p*-Xy exhibits the temperature-responsive gradual motion with heating and its recovery with cooling.

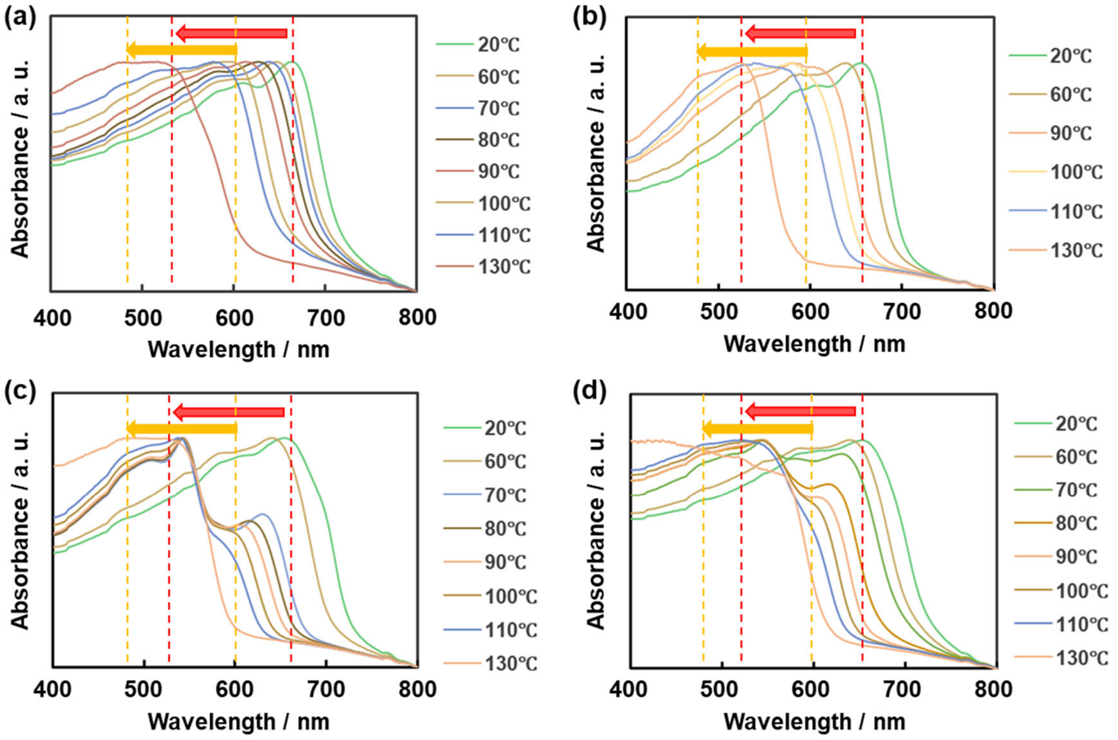

Fig. S11. Temperature-dependent UV-Vis spectroscopic changes of PAlyAm/PDA-*p*-Xy (a), PAlyAm/PDA-L-Lys (b), PMMA/PDA-*p*-Xy (c), and 4PVP/PDA-*p*-Xy (d) with heating in the range of *T* = 20 and 130 °C.

The thermoresponsive color-change properties were displayed in Fig. 5 for PAlyAm/PDA-*p*-Xy and PAlyAm/PDA-L-Lys and Fig. S5 in the ESI for PMMA/PDA-*p*-Xy and 4PVP/PDA-*p*-Xy. The temperature dependent changes of the UV-Vis spectra were listed to compare the changes in the effective conjugation length (Fig. S11). The similar temperature-dependent shift of the spectra were observed for PAlyAm/PDA-*p*-Xy and PAlyAm/PDA-L-Lys (Fig. S11a,b). The detailed explanations were described in the main text.

PMMA/PDA-*p*-Xy and 4PVP/PDA-*p*-Xy showed the absorption maxima at 680 and 600 nm at 20 °C, similar to those of PAlyAm/PDA-*p*-Xy and PAlyAm/PDA-L-Lys (the red and orange dashed lines and arrows in Fig. S11c,d). However, the spectroscopic changes with heating showed the different behavior compared with those of PAlyAm/PDA-*p*-Xy and PAlyAm/PDA-L-Lys. PAlyAm/PDA-*p*-Xy and PAlyAm/PDA-L-Lys exhibited the gradual shift to the shorter wavelength region (Fig. S11a,b). In contrast, the absorption maximum 600 nm transferred to the shorter wavelength region around 525 and 485 nm at 70 °C for PMMA/PDA-

p-Xy and 80 °C for 4PVP/PDA-*p*-Xy (Fig. S11c,d). Simultaneously, the absorption maximum around 680 nm showed the gradual shift to the shorter wavelength region. These results indicate that the matrix polymers have effects on the effective conjugation length coupled with the motion of the PDA main chain.

Mechanical stability of the PAlyAm/PDA-*p*-Xy coating

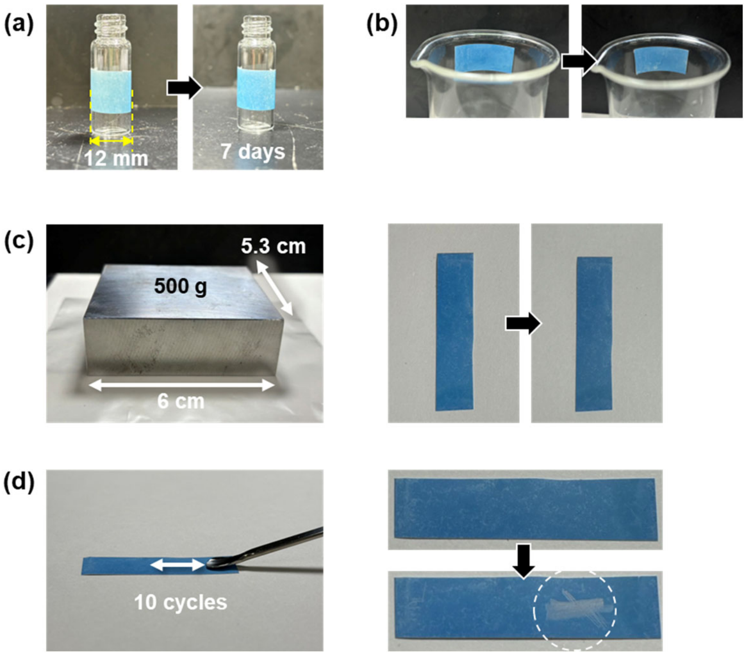

Fig. S12. Photographs of the PAlyAm/PDA-*p*-Xy coated sticker before (left panels) and after (right panels) bending (a), vibrating (b), compressing (c), and shearing (d).

The PAlyAm/PDA-*p*-Xy coated sticker was pasted on the outer wall of a glass bottle with 12 mm in diameter (Fig. S12a). After seven days, the color change to red was not observed even in the continuous bended state. The PAlyAm/PDA-*p*-Xy coated sticker was pasted on the inner wall of a glass beaker 50 cm^3 in volume (Fig. S12b). After pouring purified water at the level lower than the sticker, the sonication was carried out using an ultrasound homogenizer for 10 min. No color change was observed. The compression stress 1.57 kPa was applied to the sticker using a metal block for 1 h (Fig. S12c). The color was not changed by the compression stress. The frictional stress was applied using a spatula by hand (Fig. S12d). Although the coating slightly peeled off, the color was not changed. In this manner, the color change was not induced by the mechanical stresses.